J. Fluid Mech. (2010), *vol.* 656, *pp.* 205–222.
doi:10.1017/S0022112010001138

A model for the pinch-off process of the leading vortex ring in a starting jet

L. GAO† AND S. C. M. YU

Thermal and Fluids Engineering Division, School of Mechanical and Aerospace Engineering, Nanyang Technological University, Singapore 639798

(Received 25 June 2009; revised 28 February 2010; accepted 1 March 2010; first published online 21 May 2010)

Modifications have been made to an analytical model proposed by Shusser & Gharib (*J. Fluid Mech.*, vol. 416, 2000*b*, pp. 173–185) for the vortex ring formation and pinch-off process in a starting jet. Compared with previous models, the present investigation distinguishes the leading vortex ring from its trailing jet so as to consider the details of the pinch-off process in terms of the properties of the leading vortex ring, which are determined by considering the flux of kinetic energy, impulse and circulation from the trailing jet into the leading vortex ring by convective transportation. A two-stage process has been identified before the complete separation of the leading vortex ring from its trailing jet. The first stage involves the growth of the leading vortex ring by absorbing all the ejected fluid from the nozzle until certain optimum size is achieved. The second stage is characterized by the appreciable translational velocity of the leading vortex ring followed by a trailing jet. The leading vortex ring is approximated as a Norbury vortex ring with growing characteristic core radius ε such that dimensionless energy α, as well as its translational velocity and penetration depth, can be estimated. By applying the Kelvin–Benjamin variational principle, the pinch-off process is signified by two time scales, i.e. the formation number, which indicates the onset of the pinch-off process, and the separation time, which corresponds to the time when the leading vortex ring becomes physically separated from the trailing jet and is therefore referred to as the end of the pinch-off process. The effect of nozzle geometry, i.e. a straight nozzle or a converging nozzle, has also been taken into account by using different descriptions of the growth of the trailing jet. The prediction of the formation number and the characteristics of the vortex ring are found to be in good agreement with previous experimental results on starting jets with straight nozzles and converging nozzles, respectively.

1. Introduction

Previous experimental investigations of vortex rings made use of a piston to drive a column of fluid out to the surrounding environment (see e.g. Maxworthy 1977, Weigand & Gharib 1997 and many others). The reviews of Shariff & Leonard (1992) and Lim & Nickels (1995) provided a good discussion of properties of vortex ring at different stages and circumstances of its development, e.g. its formation, evolution, stability and interaction. Among its several interesting features, the detachment (or pinch-off) of the leading vortex ring from the trailing jet was of fundamental interest to many researchers. Gharib, Rambod & Shariff (1998) discovered that the leading

† Email address for correspondence: GA0001EI@ntu.edu.sg

vortex ring would start to pinch off from the trailing jet when the piston had discharged the column of fluid at stroke length $L(t)$ equal to four jet exit diameters ($4.0D$). The dimensionless stroke length $L(t)/D = U_p t/D$ is defined as the formation time t^*, where U_p is the average piston velocity. If the piston stops before $L/D = 4.0$, all the discharged fluid would be absorbed into the leading vortex ring. This critical formation time is commonly referred to as the 'formation number'. Existence of the universal formation number in the range of 3.6–4.5 for starting jets, with various exit geometries, velocity programmes, and Reynolds numbers, was demonstrated to be the outcome of the Kelvin–Benjamin variational principle, which states that for a steady vortex ring, the kinetic energy of impulse-preserving rearrangements of the vorticity field by an arbitrary solenoidal velocity field is maximum. As such, Gharib *et al.* (1998) suggested that the formation number could be identified as the time when the starting jet is no longer able to supply energy at the rate compatible with this energy requirement.

The physical implication of the formation number should be that, for the starting jet with maximum stroke ratio (L_m/D), which is the total stroke length a piston travels before it stops, normalized by the nozzle diameter, greater than the formation number, its flow field would consist of a leading vortex ring followed by a trailing jet. The maximum circulation the vortex ring can obtain should be equal to those emanating from the nozzle exit plane up to the formation number. However, it should be noted that the leading vortex ring might not be physically detached from its trailing jet at the formation number. The fluid in the trailing jet discharged before the formation number would continue to be absorbed by the growing vortex ring, and gradually separate from those discharged after the formation number at a later time, while the fluid discharged after the formation number would be left behind and form part of the trailing jet. The whole pinch-off process is illustrated schematically in figure 1. Similarly, Gharib *et al.* (1998) also suggested that the pinch-off process was not a sudden process and its completion might take up to two formation time units. Understanding of the pinch-off process is important to evaluation of the analytical models proposed so far for the vortex ring formation.

Theoretically, pinch-off could be considered as a relaxation process of the leading vortex ring to an equilibrium state. A model developed by Mohseni & Gharib (1998) determined the formation number by the intersection of two curves obtained from matching bulk hydrodynamic quantities (kinetic energy, impulse and circulation) with those quantities for Norbury's family of vortex rings (Norbury 1973). They utilized the slug model for the properties of the total jet, and considered them to be those of the leading vortex ring. Two equations were then obtained by equating these quantities for the slug model with corresponding quantities in the Norbury vortices. The value of the formation number was found to be between 3 and 4.5, consistent with results obtained from experiments (Gharib *et al.* 1998; Pawlak *et al.* 2007) and simulations (Rosenfeld, Rambod & Gharib 1998; Zhao, Frankel & Mongeau 2000) for the starting jet with a straight nozzle configuration. According to the description of the pinch-off process, the formation number predicted by their model should correspond to the beginning of the pinch-off process (figure 1*a*) since they mainly focused on the characteristics of the resulting vortex ring and not on the generation process.

Shusser & Gharib (2000*a*) also modelled the vortex ring formation by using a kinematic hypothesis that the vortex ring completes its formation and pinches off from its trailing jet when the translational velocity of the vortex ring becomes equal to the jet flow velocity near the ring. The translational velocity of the leading vortex ring was estimated by the properties of Norbury vortices, and the local trailing jet velocity

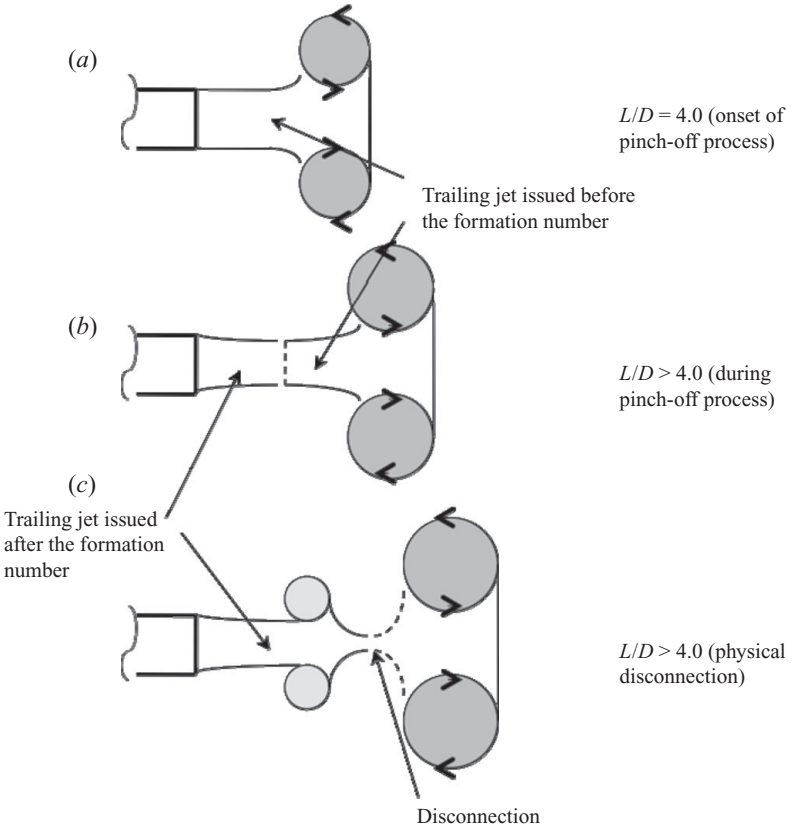

FIGURE 1. Illustration of the pinch-off process in a starting jet with $L_m/D > 4$. In real flow, the trailing jet is continuous. The dashed line and disconnection is only used to distinguish fluids issued before and after the formation number.

was related to the piston velocity via conservation of mass. The dynamic properties of the vortex ring were also approximated by those of the total jet using the slug model. By comparing the vortex ring velocity with the trailing jet velocity near the ring, they derived the limiting value of the dimensionless energy $\alpha_{lim} = 0.31$, which matches well the experimental value $\alpha_{lim} = 0.33$ (α will be defined in § 3.2). Thus, they suggested that the dynamical (based on Kelvin–Benjamin variational principle) and kinematic approaches (based on comparison of the velocities) are equivalent.

Although the basic perspectives of above models were different, both bore an assumption that, before the onset of the pinch-off process, all fluid discharged from the nozzle exit was regarded as the leading vortex ring, so that the properties of the vortex ring could be estimated by the slug model. In other words, neither model distinguished the leading vortex ring and the trailing jet before the pinch-off. Hence, the approaches of Mohseni & Gharib (1998) and Shusser & Gharib (2000*a*) may only be capable of predicting the time at which the dynamic properties provided by the generator become equal to the maxima that the leading vortex ring could attain, rather than the time at which the leading vortex ring actually acquires its maximum circulation and separates from the trailing jet.

It is important to realize that the universal formation number around 4.0 may only be applicable to starting jets that can be characterized by a sufficiently large

stroke ratio, a sufficiently high Reynolds number and sufficiently thin shear layers produced by the ejection, such as those produced by piston/cylinder arrangement with a straight nozzle (Mohseni, Ran & Colonius 2001). The formation number, however, might vary within the range from 1.0 to 5.0 with different generator configurations. For example, the formation number could be reduced to around 2.0 in experiment for the starting jet with a converging nozzle, which contracted smoothly and gradually with cross-section area contraction ratio of 52 : 1, to avoid the formation of Gortler vortices (Yu, Ai & Law 2007; Gao *et al.* 2008). With very thick shear layers produced by parabolic velocity profile at the nozzle exit plane, the formation number could even be reduced to around 1.0 (Rosenfeld *et al.* 1998; Zhao *et al.* 2000). In this paper, efforts have been made to elucidate the differences in formation number between starting jets with the commonly used straight nozzle and the converging nozzle with small convergence angle, in terms of the development of the trailing jet.

A similar flow structure was found in a starting buoyant plume (Turner 1962), which consists of a 'cap', analogous to the leading vortex ring, and a 'stem', which is the same as the trailing jet in the starting jet. Based on the structure of the starting buoyant plume, a two-stage model was proposed by Shusser & Gharib (2000*b*) to investigate the formation of vortex rings in the cap of the plume. The first stage of the process is the initial formation of the ring-like structure in the plume cap. The flow field consists only of a forming vortex ring. During the second stage, continuing action of the heat source creates a rising flow of the lighter fluid (the stem of the plume) following the ring (the cap of the plume). The flux from the stem into the ring continues until the latter has grown large enough to pinch off. So it is noted that the evolutions of the 'cap' and the 'stem' of the starting plume are considered separately in the second stage. Due to the similarity between jet and buoyant plume, this approach was adopted for the starting jet in the present investigation.

In this paper, we focus on elucidating the physical process of pinch-off in starting jets by a two-stage model, which takes into account the difference between the leading vortex ring and its trailing jet. The next section will explain the physical situation and the formulation in the model for both the straight nozzle type and the converging nozzle type of the piston/cylinder generator. It is followed by discussion of the properties of the leading vortex ring calculated by the model, and comparison with experimental results obtained by various researchers. The paper ends with brief concluding remarks.

2. Process of the leading vortex ring formation and pinch-off

In our model, the initial leading vortex ring generated by rolling up of the separated cylindrical shear layer would absorb all the fluid issued from the nozzle exit. The leading vortex ring growth is dominated by its radial expansion but it does not leave the nozzle exit plane until an optimum size of the vortex ring is reached. Then a transition from vortex ring radial expansion to axial translation distinguishes the development in Stage II from that in Stage I. During Stage II, as the leading vortex ring travels downstream, a trailing jet begins to appear and continuously feeds the vortex ring with vorticity, momentum and energy until pinch-off occurs. The detailed formation and pinch-off process is shown schematically in figure 2.

2.1. *Stage I: initial generation of the leading vortex ring*

First, we assume that the piston reaches a constant velocity U_0 immediately after the jet was initiated from a nozzle with exit diameter of D. The first stage is the formation

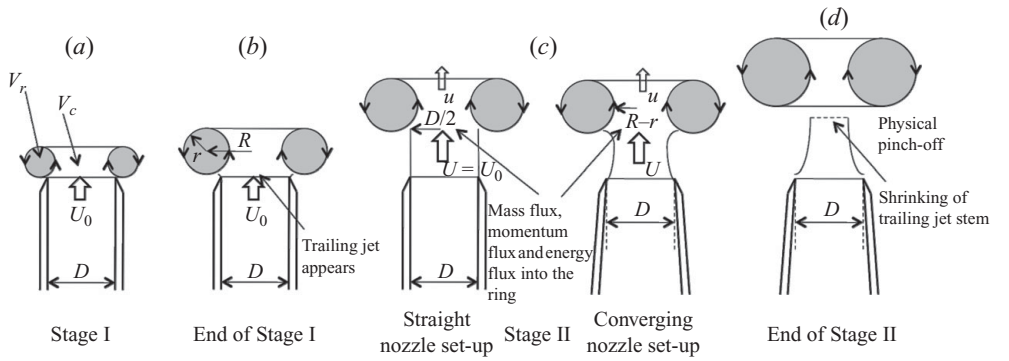

FIGURE 2. Sketch of the vortex ring evolution in the starting jet.

of vortex ring by fluid discharged with an initial momentum. The vortex ring grows rapidly in size by absorbing all of the fluid ejected from the nozzle, but it does not translate appreciably. It has been observed in experiments of Didden (1979) and Weigand & Gharib (1997) that no motion in the axial direction was noticeable until a slightly large-ring diameter was reached. Based on their experimental observations, we specify $D_r = 1.08D$ as the condition for the end of Stage I, because it is difficult to define its duration analytically. Due to the slow translation of the vortex ring, it is reasonable to make the assumption that no trailing jet appears. Moreover, recent flow visualization by Olcay & Krueger (2008) had shown that during the onset of jet ejection, the volume of entrained ambient fluid would be much less than the volume of the ejected fluid from the nozzle. The entrainment effect is therefore not considered in modelling at Stage I.

As illustrated in figure 2(*a*), the fluid discharged through the nozzle exit consists of a forming vortex ring (in light grey) and a central part. The volume of the vortex ring V_r and the volume of the central part V_c can be calculated by integration as

$$V_r = 2\pi^2 R r^2, \tag{2.1a}$$

$$V_c = 2\pi R^2 r - \pi^2 R r^2 + \tfrac{4}{3}\pi r^3. \tag{2.1b}$$

The total volume V_t discharged from the nozzle exit can be regarded as a column of fluid with the height of the stroke length and the base area of the nozzle exit, namely

$$V_t = \tfrac{1}{4}\pi D^2 L. \tag{2.1c}$$

Since the entrainment effect is negligible during Stage I, the ejected volume should be conserved, which results in

$$\tfrac{1}{4}\pi D^2 L = 2\pi^2 R r^2 + 2\pi R^2 r - \pi^2 R r^2 + \tfrac{4}{3}\pi r^3. \tag{2.2}$$

Here, R is the radius of the leading vortex ring, and r is the radius of the vortex ring core. At this stage, the sufficiently small size of the vortex ring core, in which the vorticity is confined, makes it reasonable to approximate the dimensionless mean core radius of the Norbury family of vortex rings as $\varepsilon \approx r/R$. The exact definition and implication of the mean core radius ε will be discussed in Stage II.

As the vortex ring grows, both R and r would increase with time. Since the vortex ring at the initial stage has a smaller core size compared to the nozzle diameter, the roll-up of vortex sheet at the nozzle edge can be approximated as a self-similar

inviscid process in two dimensions. Based on the similarity law for axisymmetric jets discussed by Saffman (1978), the growth of the radius of the vortex ring R can be expressed as

$$R/D = 0.5 + Ct^{*2/3}, \tag{2.3}$$

where coefficient C is equal to 0.17 from the experimental result of Didden (1979). Therefore, the end of Stage I can be found to be at $t^* = 0.12$ from the criterion that $D_r = 1.08D$ at end of Stage I. It shows that Stage I is indeed a very transient period.

In summary, (2.2) and (2.3) describe the initial development of the starting jet in Stage I ($0 < t^* < 0.12$). The properties of the vortex ring and the jet, such as ring size, total volume and dynamic properties, at the end of Stage I would be used as the initial conditions for the calculation in Stage II. Note that difference in generator configuration is not considered in Stage I, since its effect in this short period would not significantly influence the further development of the starting jet.

2.2. *Stage II: growth and pinch-off of the leading vortex ring*

After the initial formation of the leading vortex ring, the development of the starting jet is characterized by the appearance of a trailing jet behind the translating leading vortex ring. The growth of the vortex ring is supported by the flux from the trailing jet until it pinches off. Thus, the total kinetic energy, impulse and circulation delivered by the jet cannot be regarded as those only for the leading vortex ring due to the existence of the trailing jet. Those quantities of the leading vortex ring, however, may be estimated by the flux from the trailing jet into the ring.

The local trailing jet velocity U near the ring can be related to the piston velocity U_0 based on the following assumptions. First, we assume that the trailing jet can be approximated as a one-dimensional axisymmetric flow and entrainment of ambient fluid in the trailing jet is negligible. Second, for two configurations of the jet generator, the difference in the growth of the trailing jet must be considered. For the starting jet with the straight nozzle configuration (on the left of figure 2*c*), the mass and momentum along the trailing jet should be constant, based on the approximation of one-dimensional flow without entrainment. Therefore, it can be obtained that the trailing jet velocity U_{sn} and its radius b_{sn} would not change along the trailing jet, resulting in

$$U_{sn} = U_0, \quad b_{sn} = \frac{D}{2}. \tag{2.4a}$$

Henceforth, subscript '*sn*' denotes quantities only for the straight nozzle configuration, and '*cn*' denotes the quantities only for the converging nozzle configuration. It is consistent with the flow visualization results of Olcay & Krueger (2008). They showed that the radius of the trailing jet is almost constant before the appearance of the secondary vortices in the trailing jet. On the other hand, for the starting jet with the converging nozzle set-up, the trailing jet tends to shrink due to the converging streamlines. It should be noted that the concept of a converging nozzle in the model should be restricted to nozzles with small convergence angle. To take the shrinking trend into account, the radius of the trailing jet b_{cn} close to the ring is approximated by the difference between ring radius and core radius ($R - r$), as shown on the right of figure 2(*c*). In fact, the size of the core r would normally grow faster than the size of the ring R (see Hettel *et al.* 2007, figure 19). Then, by applying conservation of mass in the trailing jet, we obtain

$$U_{cn} = \frac{D^2}{4R^2(1-\varepsilon)^2}U_0, \quad b_{cn} = R - r. \tag{2.4b}$$

In order to predict the variation of dynamic properties (kinetic energy, impulse and circulation) of the leading vortex ring at Stage II, their flux from the trailing jet into the leading vortex ring needs to be estimated. Heeg & Riley (1997) showed that the total circulation rate $\mathrm{d}\Gamma_{total}/\mathrm{d}t$ is actually slightly above the slug model value $\mathrm{d}\Gamma_{total}/\mathrm{d}t = 0.5U_0^2$ at large times, owing to boundary-layer growth inside the nozzle. Didden (1979) found that the best approximation of the vorticity flux through the nozzle exit was

$$\frac{\mathrm{d}\Gamma_{total}}{\mathrm{d}t} = 0.57U_0^2 \quad \text{for } t^* > 0.6. \tag{2.5}$$

Equation (2.5) can be regarded as the rate of the total circulation provided by the jet. With regard to the leading vortex ring, its circulation is derived from the vorticity flux into the ring. As for the slug model at the nozzle exit plane, one can derive the vorticity flux near the rear of the leading vortex ring as

$$\frac{\mathrm{d}\Gamma}{\mathrm{d}t} = \int_0^\infty (U-u)\omega_\theta \mathrm{d}r \approx \frac{1}{2}U^2 - Uu, \tag{2.6}$$

where u is the translational velocity of the leading vortex ring, and would increase as the ring grows. For impulse and energy, their flux from the trailing jet are given by

$$\frac{\mathrm{d}I}{\mathrm{d}t} = \pi(R-r)^2\rho U(U-u), \tag{2.7}$$

$$\frac{\mathrm{d}E}{\mathrm{d}t} = \frac{1}{2}\pi(R-r)^2\rho U^2(U-u). \tag{2.8}$$

For the flux of dynamic properties, no subscript is used in (2.6)–(2.8) because they are valid for both the straight nozzle and converging nozzle configurations.

Finally, as confirmed by many investigations (Mohseni *et al.* 2001; Gao *et al.* 2008), the leading vortex ring can be approximated as a member of Norbury's family of vortex rings, which is characterized by the dimensionless mean core radius ε. Accordingly, the translational velocity of the leading vortex ring u is given by Fraenkel's second-order formulas (Fraenkel 1972) as

$$u = B\sqrt{\frac{\rho\Gamma^3}{\pi I}} \quad \text{with } B = \frac{1}{4}\sqrt{1+\frac{3}{4}\varepsilon^2}\left[\ln\frac{8}{\varepsilon} - \frac{1}{4} + \frac{3\varepsilon^2}{8}\left(\frac{5}{4} - \ln\frac{8}{\varepsilon}\right)\right]. \tag{2.9}$$

For the vortex rings with small cross-section ($\varepsilon < 0.5$), the accuracy of Fraenkel's approximation has been estimated to be very good, with the error less than 2 % (Shusser *et al.* 2006). The impulse and energy of the leading vortex ring can be expressed in terms of its circulation and size, i.e.

$$I = \rho\pi\Gamma R^2\left(1+\frac{3}{4}\varepsilon^2\right), \tag{2.10}$$

$$E = \frac{1}{2}\rho R\Gamma\left[\ln\frac{8}{\varepsilon} - \frac{7}{4} + \frac{3}{8}\varepsilon^2\ln\frac{8}{\varepsilon}\right]. \tag{2.11}$$

As the growth of the leading vortex ring, the value of the dimensionless core radius ε would increase during Stage II.

Based on (2.4*a*, *b*) and (2.6)–(2.11), the flow development during the second stage can be determined. Dimensionless variables are introduced as

$$\left.\begin{aligned} t^* = \frac{tU_0}{D},\ \bar{R} = \frac{R}{D},\ \bar{r} = \frac{r}{D},\ \bar{b} = \frac{b}{D},\ \varepsilon = \frac{r}{R},\ \bar{U} = \frac{U}{U_0},\ \bar{u} = \frac{u}{U_0}, \\ \bar{I} = \frac{I}{\rho\pi D^3 U_0},\ \bar{E} = \frac{E}{1/2(\rho\pi D^3 U_0^2)},\ \bar{\Gamma} = \frac{\Gamma}{U_0 D}. \end{aligned}\right\} \tag{2.12}$$

Substituting (2.9) into (2.6)–(2.8), and applying normalization (2.12) to the resultant equations (2.6)–(2.8), (2.10) and (2.11), we obtained a system of differential-algebraic equations:

$$\frac{\mathrm{d}\bar{I}}{\mathrm{d}t^*} = \bar{b}^2\bar{U}\left(\bar{U} - B\sqrt{\frac{\bar{\Gamma}^3}{\pi^2\bar{I}}}\right), \tag{2.13}$$

$$\frac{\mathrm{d}\bar{E}}{\mathrm{d}t^*} = \bar{b}^2\bar{U}^2\left(\bar{U} - B\sqrt{\frac{\bar{\Gamma}^3}{\pi^2\bar{I}}}\right), \tag{2.14}$$

$$\frac{\mathrm{d}\bar{\Gamma}}{\mathrm{d}t^*} = \frac{1}{2}\bar{U}\left(\bar{U} - B\sqrt{\frac{\bar{\Gamma}^3}{\pi^2\bar{I}}}\right), \tag{2.15}$$

$$\bar{I} = \bar{\Gamma}\bar{R}^2\left(1 + \frac{3}{4}\varepsilon^2\right), \tag{2.16}$$

$$\bar{E} = \frac{\bar{R}\bar{\Gamma}^2}{\pi}\left(\ln\frac{8}{\varepsilon} - \frac{7}{4} + \frac{3}{8}\varepsilon^2\ln\frac{8}{\varepsilon}\right). \tag{2.17}$$

By substituting normalized equation (2.4*a*, *b*) into (2.13)–(2.17) for starting jets with straight and converging nozzles, respectively, the properties of the leading vortex ring were solved by using the conditions obtained at the end of Stage I.

3. Results and discussion

3.1. *Initial formation of the leading vortex ring*

By solving (2.2) and (2.3), the radius of the leading vortex ring core r can be obtained as functions of formation time t^*, as shown in figure 3. At the end of Stage I, the radius of ring core r was calculated to be $0.0451D$ and the dimensionless mean core radius ε is calculated to be 0.0833. The leading vortex ring is of very small core size during the initial stage of the jet development. The experiment by Didden (1979) reported that the trajectory of the vortex core varied according to the similarity law (defined in (2.3)) up to the formation time $t^* = 0.6$, which is larger than the end of Stage I defined here $t^* = 0.12$. Therefore, one may expect that the vortex ring is self-similar even when it starts translating.

Figure 3 also shows the normalized radius of the vortex core versus formation time from the similarity law (Saffman 1978) that has confirmed by numerous experimental studies. Hettlel *et al.* (2007) confirmed the similarity law that the dependence of the radius of the vortex spiral r/D on formation time t^* was approximately equal to $0.125t^{*2/3}$, while the prediction in present model shows a slightly greater growth rate. The deviation from the simulation is probably due to the simplified geometry of the vortex ring in this model, which tends to underestimate the volume of the centre part V_c and results in greater volume of the vortex ring V_r and bigger ring core size.

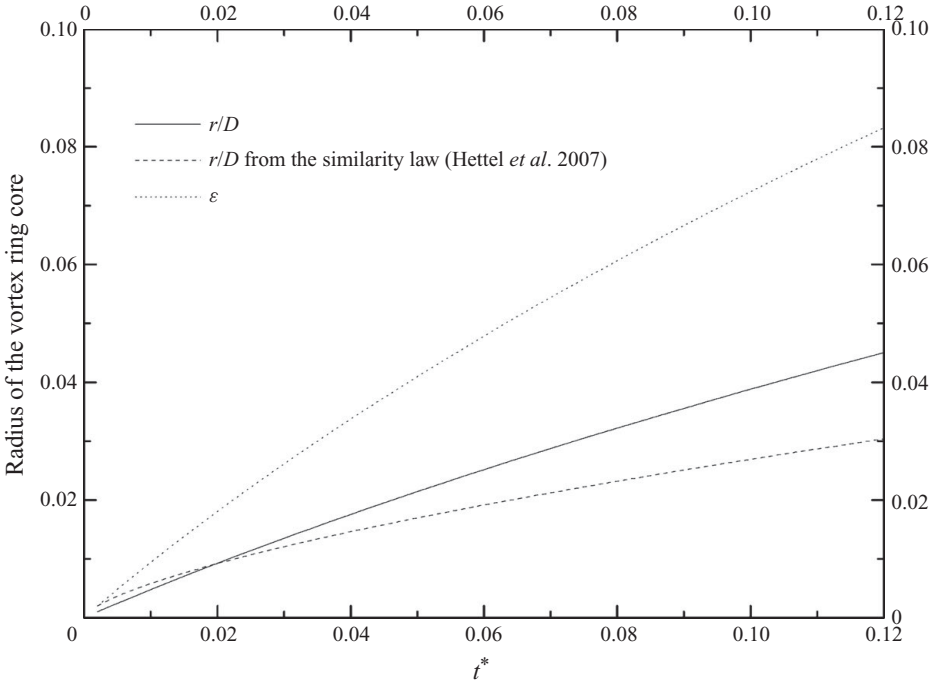

FIGURE 3. Growth of the radius of the leading vortex ring core during Stage I, and comparison with the similarity law (see Hettel *et al.* 2007).

Because the first stage is identified as a very transient period, it is appropriate to involve the overpressure effect on the properties of the leading vortex ring during this period. It has been reported that the slug model consistently underestimates the total circulation and energy by a near-constant for the impulsively starting jet (Didden 1979; Krueger 2005; Yu *et al.* 2007). The error in slug model arises primarily from neglecting the overpressure at the nozzle exit plane, which developed as a result of the unsteady flow initiation and distorted the velocity profile at the nozzle exit. For nozzle configuration, Krueger (2005) proposed an overpressure correction Γ_p to the circulation prediction by slug model Γ_U for small formation time as $\Gamma_p/(U_0 D) \approx 1/\pi$. In order to obtain the circulation of vortex ring at the end of Stage I, the overpressure correction is included as

$$\bar{\Gamma}_{end\_I} = (\bar{\Gamma}_U)_{t^*=0.12} + (\bar{\Gamma}_P)_{t^*=0.12} \approx \left(\frac{1}{2}t^*\right)_{t^*=0.12} + \frac{1}{\pi} = 0.3783. \tag{3.1}$$

Moreover, we assume the initial vortex ring at the end of Stage I can be approximated as a Norbury vortex, so as to enable the smooth transition of the properties of the ring form Stage I to Stage II. Therefore, the energy and impulse of the leading vortex ring at the end of Stage I are calculated from (2.16) and (2.17) by substituting in the value of circulation $\bar{\Gamma} = 0.3783$, mean core radius $\varepsilon = 0.0833$ and ring radius $\bar{R} = 0.5414$. In summary, the initial conditions for Stage II are

$$\left.\begin{array}{c} \bar{I}_{end\_I} = 0.1114, \quad \bar{E}_{end\_I} = 0.0697, \\ \bar{\Gamma}_{end\_I} = 0.3783, \quad \bar{R}_{end\_I} = 0.5414, \quad \varepsilon_{end\_I} = 0.0833. \end{array}\right\} \tag{3.2}$$

It should also be noted that, apart from calculating the end state, we do not include any dynamical aspect of the vortex sheet roll-up in this stage. Instead, the model relies

on conservation of the ejected volume in combination with the theoretical similarity law with the empirical fitted coefficient.

3.2. *Evolution of the leading vortex ring during the pinch-off process*

3.2.1. *Formation number and separation time*

By solving the system of equations (2.13)–(2.17) with corresponding initial conditions from (3.2), we can predict the trajectory, size, and dynamic properties of the leading vortex ring in Stage II until it pinches off from the trailing jet. First, the onset and end of the pinch-off process should be identified before discussing the evolution of the leading vortex ring. Since the end of Stage II is determined by the separation time when the leading vortex ring physically detaches from the trailing jet, the model fails after Stage II when the flux into the leading vortex ring from the trailing jet no longer exists. Mohseni *et al.* (2001) pointed out that the formation process is governed by two dimensionless parameters that are formed from the three integrals of motion (kinetic energy, impulse and circulation) and the translational velocity of the leading vortex ring, i.e. the dimensionless energy and circulation. The dimensionless energy α is defined as

$$\alpha = \frac{E}{\sqrt{\rho I \Gamma^3}} = \frac{\bar{E}}{2}\sqrt{\frac{\pi}{\bar{I}\bar{\Gamma}^3}}. \tag{3.3}$$

Therefore, the pinch-off process of the leading vortex ring can be quantified in terms of the variation of the dimensionless energy, discussed as follows.

Based on the Kelvin–Benjamin variational principle, Gharib *et al.* (1998) suggested that the onset of the pinch-off process, by definition coinciding with the formation number, can be determined by the time when the total dimensionless energy α_{total} provided by the jet generator decreases beyond a certain limiting value α_{lim}. It has been observed experimentally by Gharib *et al.* (1998), Allen & Naitoh (2005) and Gao *et al.* (2008) that for the vortex rings in the jet with constant velocity programme, $\alpha_{lim} = 0.33 \pm 0.05$ without a clear trend for different generation mechanisms. But at the formation number, the dimensionless energy of the leading vortex ring α_{ring} should be still higher than α_{lim} since it has not obtained its maximum circulation. During the pinch-off process, as the vortex ring core thickens, α_{ring} is expected to diminish to the limiting value α_{lim}. Therefore, the criterion for determining the separation time is that the leading vortex ring completes its formation and separates from the trailing jet once the dimensionless energy of the leading vortex ring α_{ring} becomes less than the limiting value α_{lim}.

The variations of dimensionless energy α_{ring} of the leading vortex ring against formation time t^* for the converging nozzle and straight nozzle configurations are presented in figure 4. For the converging nozzle case, the dynamic properties of total jet flow are estimated by the slug model with a correction on the circulation given in (2.5) as

$$\bar{I}_{total} = \bar{I}_{end\_I} + \tfrac{1}{4}(t^* - 0.12), \tag{3.4}$$

$$\bar{E}_{total} = \bar{E}_{end\_I} + \tfrac{1}{4}(t^* - 0.12), \tag{3.5}$$

$$\bar{\Gamma}_{total} = \bar{\Gamma}_{end\_I} + 0.57(t^* - 0.12). \tag{3.6}$$

Then α_{total} is calculated from (3.3)–(3.6), and also plotted in figure 4(*a*). The formation number is predicted roughly at around 2.2. Both the total jet energy α_{total} and the formation number are consistent with the experiment of starting jets using converging

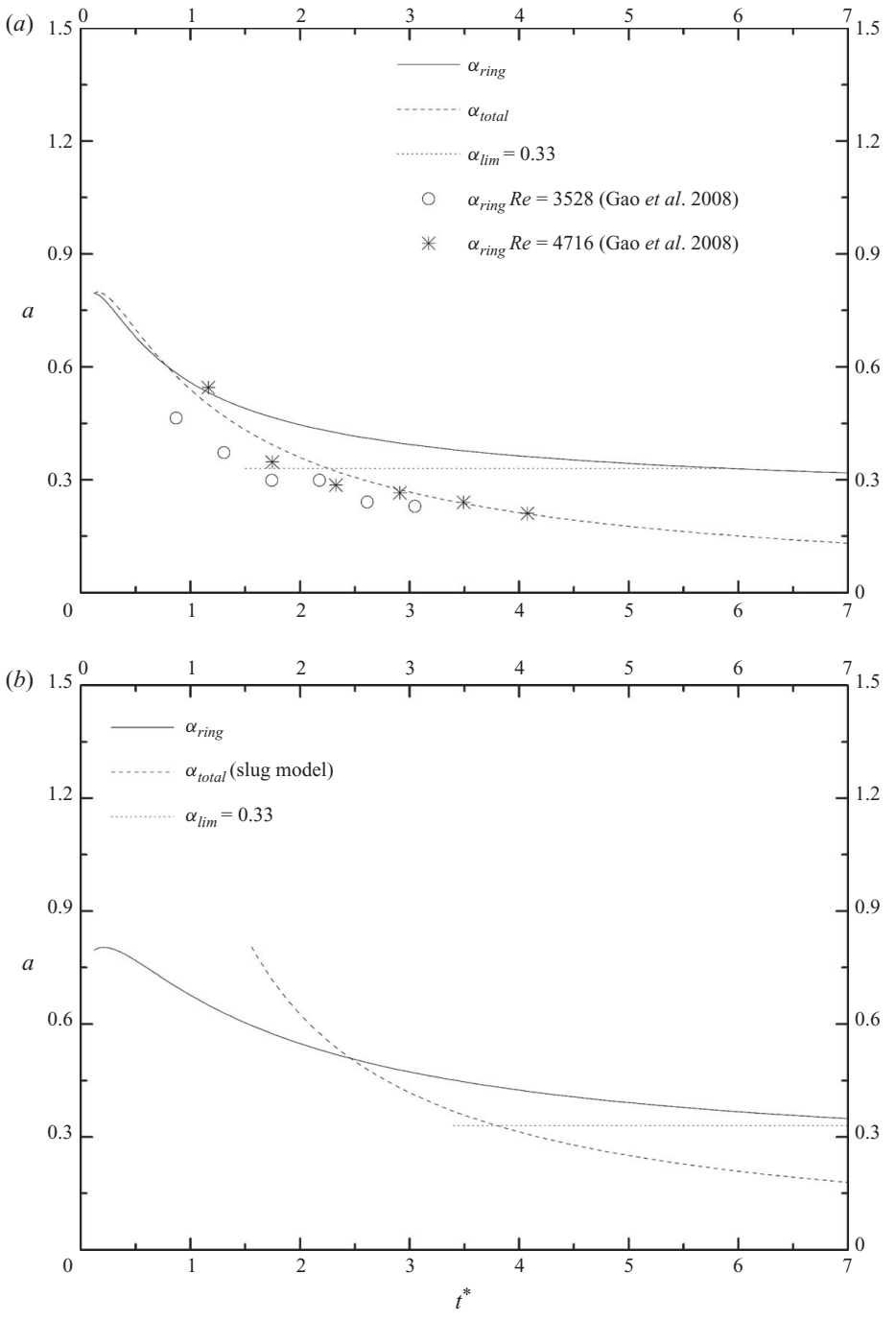

FIGURE 4. Variation of the dimensionless energy of the leading vortex ring and the total jet during Stage II for (*a*) the starting jet with a converging nozzle and (*b*) the starting jet with a straight nozzle.

nozzles by Gao *et al*. (2008) in which the formation number was found to be at about 2.2. The physical separation of the leading vortex ring occurred later on. To predict the separation time for the converging nozzle configuration, the

dimensionless energy of the leading vortex ring α_{ring} is also plotted in figure 4(*a*). At small formation time, α_{ring} is close to the total energy of the jet α_{total}. But for $t^* > 1.0$, the difference between α_{ring} and α_{total} increases because some energy provided by the jet should be left behind in the trailing jet. When approaching the end of Stage II, the rate of change of α_{ring} seems to slow down, indicating the invariant properties of the ring after it was completely formed. According to the criterion stated above, we compare the variation of α_{ring} with this limiting value α_{lim}, and estimate the value of the separation time by the intersection of ring energy curve and the limiting value. As shown in figure 4(*a*), it suggests that the separation time of the leading vortex ring is approximately at $t^* = 5.0$.

The result of the formation number and separation time for a converging nozzle suggested that at $t^* \approx 2.2$, the jet with a converging nozzle provides the fluid with energy consistent with those for the steady translating vortex ring, namely $\alpha_{total} = \alpha_{lim}$. However, part of the fluids that have not been absorbed by the vortex ring remained in the trailing jet. Because the leading vortex ring continues absorbing fluid from the trailing jet, it would approach steady state when $\alpha_{ring} = \alpha_{lim}$, and becomes totally separated from the trailing jet at $t^* \approx 5.0$, namely the separation time. That defines the whole process of vortex ring pinch-off in the starting jet with a converging nozzle.

For the straight nozzle configuration, Gharib *et al.* (1998) showed that the slug model could predict the evolution of total energy α_{total} with reasonable accuracy. The solution of the model with constant trailing jet approximation gives the variation of the dimensionless energy for the ring α_{ring}. As shown in figure 4(*b*), the predicted formation number is at about 3.9, which matches well with prior results (Gharib *et al.* 1998; Rosenfeld *et al.* 1998; Zhao *et al.* 2000). And the separation time for a straight nozzle is found to be a bit greater than 7.0. A similar phenomenon was observed by Sau & Mahesh (2007) that for a cylindrical nozzle, even if the formation number is found to be approximately 3.6, the leading vortex ring clearly pinches off from the trailing jet at around $t^* \approx 11$. By comparing figures 4(*a*) and 4(*b*) for the converging nozzle and straight nozzle configurations, the difference in the evolution of dimensionless energy and the formation number exhibits the effect of nozzle geometry on the trailing jet development as specified in § 2.2. It indicates that by modifying the condition corresponding to the generation mechanism, the current model is capable of predicting the pinch-off process in both the straight nozzle and converging nozzle configurations.

As for the Kelvin–Benjamin variational principle, it should be noted that the total dimensionless energy is usually estimated by the slug model. The dimensionless energy of the steady leading vortex ring after pinch-off usually makes use of the experimental results by Gharib *et al.* (1998). The limiting value $\alpha_{lim} = 0.33 \pm 0.05$ has been theoretically predicted by Mohseni & Gharib (1998), but the use of the slug model limits its generality for different discharging processes of the fluid from the nozzle. The properties of the leading vortex rings are functions of different rates of generation of primary and secondary vorticity. The universal value of dimensionless energy $\alpha_{ring} = 0.33$ only exists in some particular starting jets, such as those with an impulsive start, constant velocity programme, and moderate Reynolds number. By using the time-varying diameter of the jet exit, Mohseni *et al.* (2001) and Allen & Naitoh (2005) had successfully produced thick vortex rings with non-dimensional energy as low as 0.22 and 0.17, respectively. The implication of this observation, therefore, is to reveal the underlying relation between vorticity generation mechanisms and the final state of the leading vortex ring in the starting jet, under the approximation that the ring belongs to the Norbury family of vortex rings. It is a very interesting issue worth further work.

3.2.2. *Interaction between the leading vortex ring and the trailing jet*

For the converging nozzle configuration, the initial converging streamlines would lead to the decrease of the trailing jet radius and a corresponding increase in the velocity of the trailing jet. This trend is examined by the prediction of the translational velocity of the leading vortex ring and the local velocity of the jet at the rear of the vortex ring, as shown in figure 5(*a*). The translational velocity of the ring u increases with a slightly reducing slope until the separation time $t^* \approx 5.0$. The increasing translational velocity u suggests that even after the formation number $t^* = 2.2$, the vortex ring does not reach its steady state, but it is still in the formation phase by gaining momentum from the trailing jet until their physical separation. It shows in figure 5(*a*) that the variation of u only agrees well with the experimental result of Gao *et al.* (2008) at around the formation number $t^* = 2.2$, but overestimates it near the end of Stage II ($t^* \approx 5.0$). As may have been expected, the trailing jet velocity U in this model increases rapidly against time and becomes equal to about $2.1U_0$ at the end of Stage II ($t^* \approx 5.0$). On the other hand, in figure 5(*b*), the value of u for the straight nozzle configuration agrees well with those found by Gharib *et al.* (1998) and Schram & Riethmuller (2001), especially near the formation number $t^* = 4.0$.

The discrepancy in translational velocity between prediction and experimental result may be attributed to the fact that the model is not capable of taking into account the influence of the Kelvin–Helmholtz-type vortex rings forming in the trailing jet. As illustrated in a sequence of planar laser-induced fluorescence (PLIF) images in figure 3 of Yu *et al.* (2007), a noticeable feature during the vortex ring pinch-off is the formation of vortex rings in the trailing jet. Once the first trailing vortex ring is formed, it would absorb the vorticity from upstream and downstream, causing the flux of dynamic properties into the leading vortex ring to reduce. Without considering this effect, the model tends to overestimate the translational velocity of the leading vortex ring. This effect suggests that the interaction between the leading vortex ring and the trailing vortices is a crucial factor for determining the properties of the leading vortex during the pinch-off process. We would like to note that further analytical work on this instability of the trailing jet is worth studying so as to provide a more accurate description of the pinch-off process.

The prediction of the variation of the radius of the leading vortex ring and its core is presented in figure 6. The result for the converging nozzle case (figure 6*a*) shows that the radius of the ring core indeed grows faster than that of the ring. Comparison with the experimental results (Gao *et al.* 2008) implies that the model generally underestimates the growth of the vortex ring radius at small formation time, but matches well with the experimental results near the end of Stage II. In figure 6(*b*), the present model for the straight nozzle configuration shows good agreement with the growth of the size of the vortex ring, especially at the early period of the formation process. For initial development of the starting jet ($t^* < 0.6$), Didden (1979) found the growth of the vortex ring diameter given by (2.3). For further development, Liess (1978) has reported a power-law dependence of the change of ring diameter on the formation time, i.e.

$$D_{ring}/D = 1.18(t^*)^{1/5} \text{ for } 1.0 \leqslant t^* \leqslant 3.3. \tag{3.7}$$

The characteristic mean core radius in the straight nozzle jet increases rapidly during the second stage of development. Its value is found to be at about 0.45 when the leading vortex ring completes its formation at about $t^* \approx 7.0$. This value is consistent with the experimental result of the properties of the vortex ring with dimensionless energy α of 0.33. Likewise, in figure 6(*a*) for the converging nozzle case, the mean

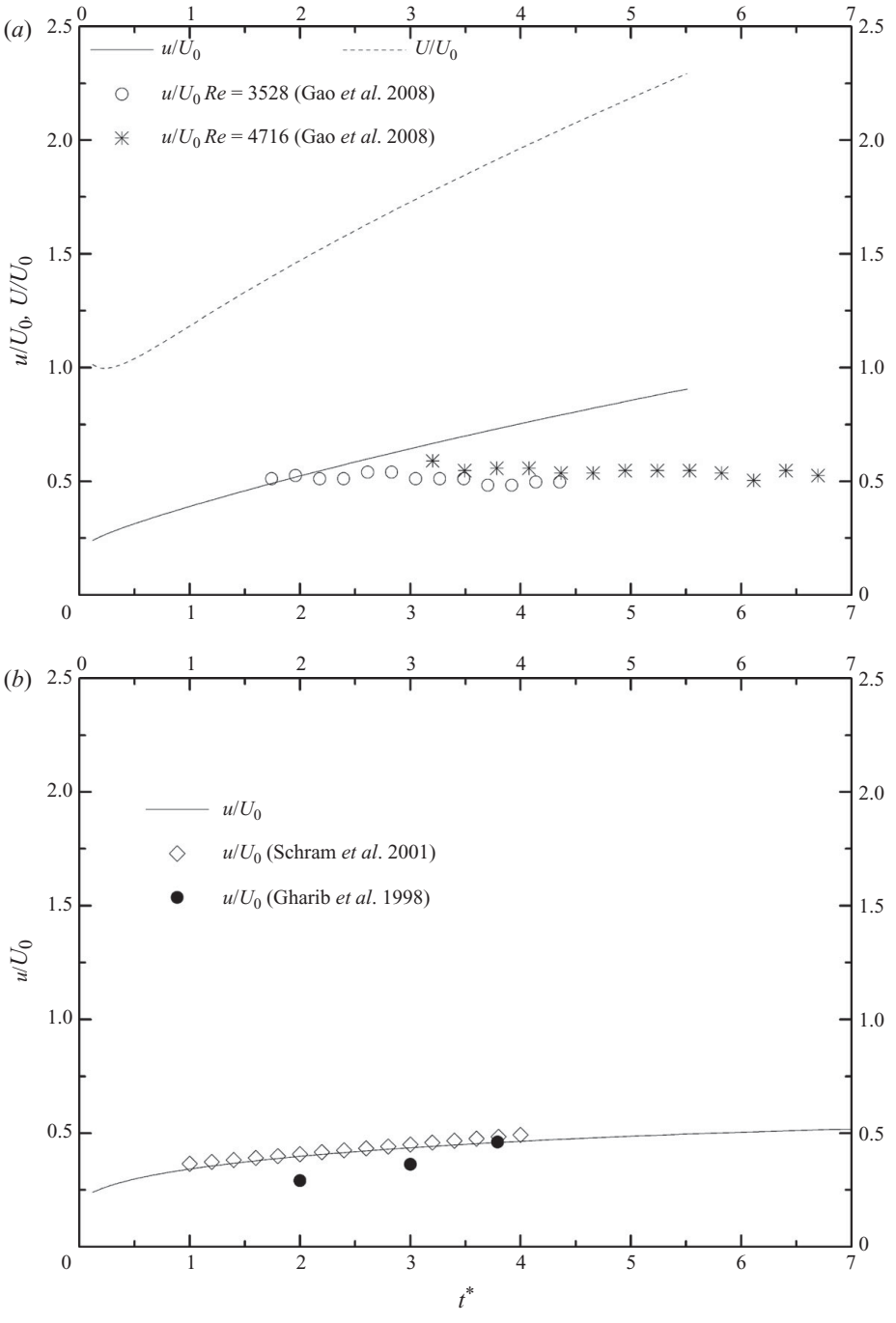

FIGURE 5. Evolution of the velocity of the trailing jet U and the leading vortex ring u for (a) the starting jet with a converging nozzle and (b) the starting jet with a straight nozzle, and the comparison with experimental results.

core radius ε also approaches the value of 0.45 at the end of the pinch-off process. It implies that the model can obtain the invariance of the properties of the leading vortex ring towards its steady state for different generator configurations.

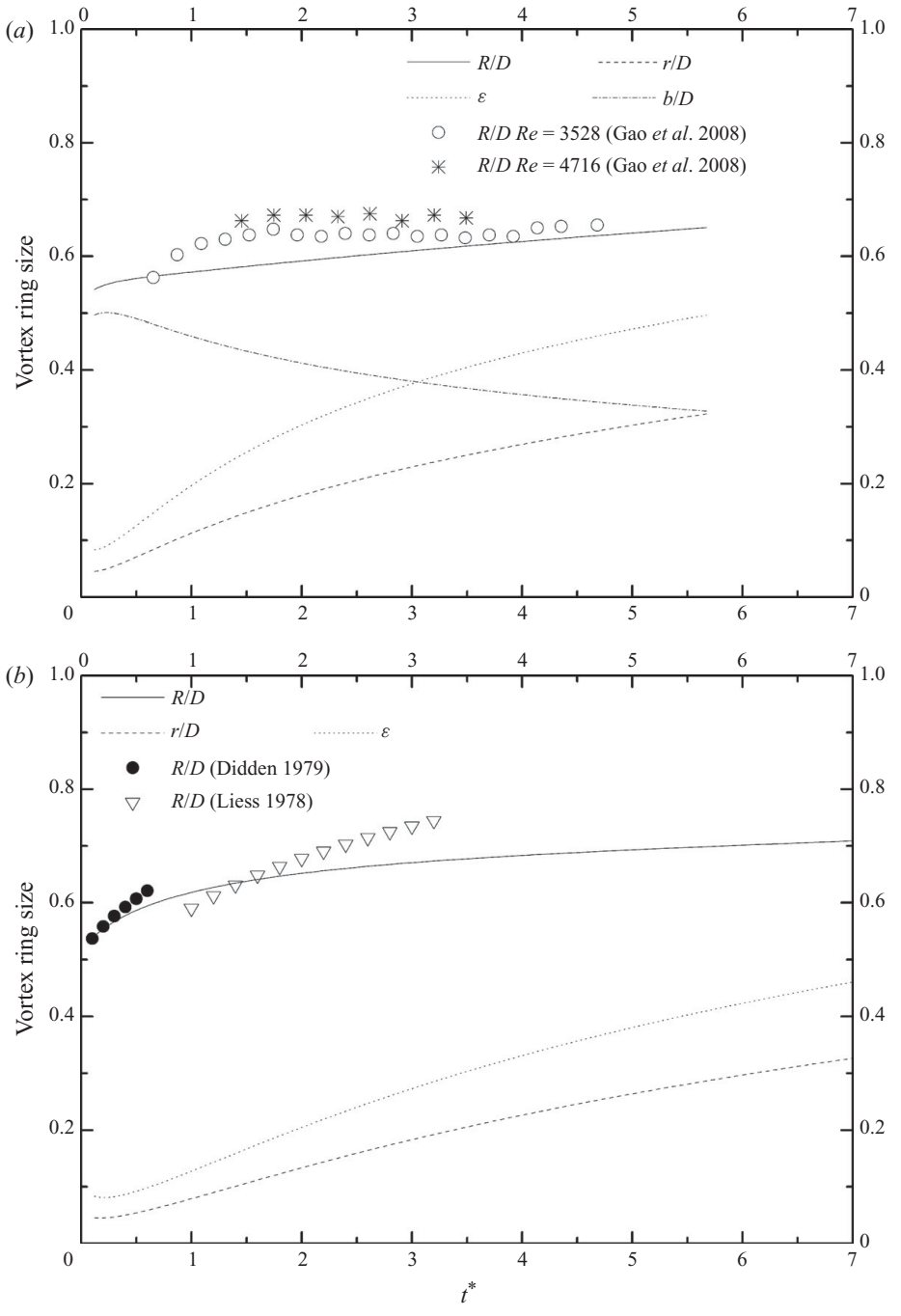

FIGURE 6. Evolution of radius of the leading vortex ring R, of the ring core r and the value of mean core radius ε for (*a*) the starting jet with a converging nozzle and (*b*) the starting jet with a straight nozzle.

3.2.3. *Penetration of jet tip*

Another interesting feature of starting jets is the penetration of the jet tip. The axial position of the vortex ring core X can be predicted by integration of the translational

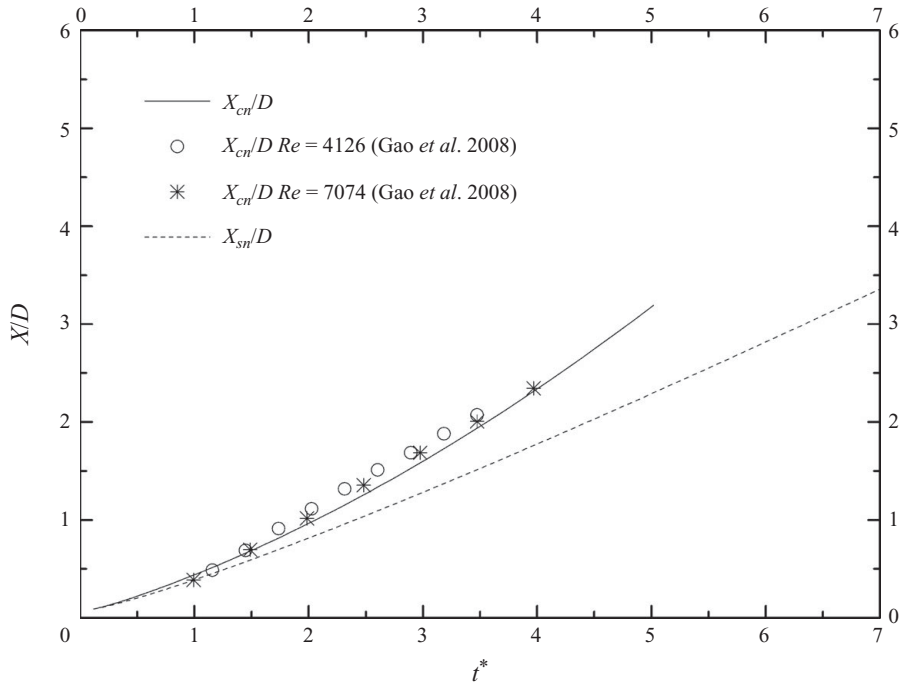

FIGURE 7. Normalized penetration of the jet tip for both the converging nozzle and straight nozzle configurations, compared with experimental results.

velocity of the ring. Based on the simplified geometry of vortex rings in this model (see figure 2), the axial position of the jet front (or jet tip) can also be derived by the core position added by the core radius r. The predicted jet penetration for both the straight nozzle and converging nozzle configurations are presented in figure 7. Due to the faster translational velocity of the leading vortex ring in the converging nozzle case, its penetration is estimated to be stronger than that in the straight nozzle case. Their curves also exhibit a varying slope during the period from the onset of the pinch-off process (when t^* equals formation number) to the end of the pinch-off process (when t^* equals separation time), approaching a steady state of the leading vortex ring. The jet penetration compares well with the experimental results for the starting jet with a converging nozzle for different Reynolds numbers (Gao *et al.* 2008).

4. Concluding remarks

An analytical model was proposed based on some modifications to the model of Shusser & Gharib (2000*b*) for starting plumes, so as to study the dynamic process of vortex ring formation and pinch-off in starting jets with different generator configurations. By altering the approximation on the growth of trailing jets, the model was capable of predicting the vortex ring pinch-off process in both starting jets generated by converging nozzles and those generated by straight nozzles. The development of the starting jet was modelled into two stages before the leading vortex ring actually pinches off from the trailing jet. By considering the existence of trailing jet during the vortex formation, the detailed vortex ring formation and pinch-off process can be elucidated by the properties of the leading vortex ring, such as the size, trajectory, velocity and dynamic properties. At Stage II, the pinch-off process

can be characterized by two time scales, i.e. formation number and separation time. By applying the Kelvin–Benjamin variational principle, the values of the formation number and the separation time for the converging nozzle case were found to be about 2.2 and 5, respectively, in good agreement with corresponding experimental results of Gao *et al.* (2008). And for the straight nozzle configuration, the separation time of a bit greater than 7.0, in combination with the formation number of 4.0 predicted by the slug model (Gharib *et al.* 1998), identifies the whole pinch-off process in starting jets with straight nozzles. In addition, comparison with previous experimental results suggests that the prediction on separation time could be improved by considering the formation of the first trailing vortex ring in the trailing jet.

Financial support from Academic Research Grant Committee and the research studentship from the School of Mechanical and Aerospace Engineering for the first author are gratefully acknowledged.

REFERENCES

Allen, J. J. & Naitoh, T. 2005 Experimental study of the production of vortex rings using a variable diameter orifice. *Phys. Fluids* **17**, 061701.

Didden, N. 1979 On the formation of vortex rings: rolling-up and production of circulation. *J. Appl. Math. Phys.* **30**, 101–116.

Fraenkel, L. E. 1972 Examples of steady vortex rings of small cross-section in an ideal fluid. *J. Fluid Mech.* **51**, 119–135.

Gao, L., Yu, S. C. M., Ai, J. J. & Law, A. W. K. 2008 Circulation and energy of the leading vortex ring in a gravity-driven starting jet. *Phys. Fluids* **20**, 093604.

Gharib, M., Rambod, E. & Shariff, K. 1998 A universal time scale for vortex ring formation. *J. Fluid Mech.* **360**, 121–140.

Heeg, R. S. & Riley, N. 1997 Simulations of the formation of an axisymmetric vortex ring. *J. Fluid Mech.* **339**, 199–211.

Hettel, M., Wetzel, F., Habisreuther, P. & Bockhorn, H. 2007 Numerical verification of the similarity laws for the formation of laminar vortex rings. *J. Fluid Mech.* **590**, 35–60.

Krueger, P. 2005 An over-pressure correction to the slug model for vortex ring circulation. *J. Fluid Mech.* **545**, 427–443.

Liess, C. 1978 Experimentelle Untersuchung des Lebenslaufes von Ringwirbeln. *Tech. Rep.* Max-Planck-Institut für Strömungsforschung, Göttingen.

Lim, T. T. & Nickels, T. B. 1995 Vortex rings. In *Vortices in Fluid Flows* (ed. S. I. Green). Kluwer.

Maxworthy, T. 1977 Some experimental studies of vortex rings. *J. Fluid Mech.* **81**, 465–495.

Mohseni, K. & Gharib, M. 1998 A model for universal time of vortex ring formation. *Phys. Fluids* **10**, 2436–2438.

Mohseni, K., Ran, H. & Colonius, T. 2001 Numerical experiments on vortex ring formation. *J. Fluid Mech.* **430**, 267–282.

Norbury, J. 1973 A family of steady vortex rings. *J. Fluid Mech.* **57**, 417–443

Olcay, A. & Krueger, P. 2008 Measurement of ambient fluid entrainment during laminar vortex ring formation. *Exp. Fluids* **44**, 235–247.

Pawlak, G., Cruz, C. M., Bazan, C. M. & Hrdy, P. G. 2007 Experimental characterization of starting jet dynamics. *Fluid Dyn. Res.* **39**, 711–730.

Rosenfeld, M., Rambod, E. & Gharib, M. 1998 Circulation and formation number of laminar vortex rings. *J. Fluid Mech.* **376**, 297–318.

Saffman, P. 1978 The number of waves on unstable vortex rings. *J. Fluid Mech.* **84**, 625–639.

Sau, R. & Mahesh, K. 2007 Passive scalar mixing in vortex rings. *J. Fluid Mech.* **582**, 449–461.

Schram, C. & Riethmuller, M. L. 2001 Vortex ring evolution in an impulsively started jet using digital particle image velocimetry and continuous wavelet analysis. *Meas. Sci. Technol.* **12**, 1413–1421.

Shariff, K. & Leonard, A. 1992 Vortex rings. *Ann. Rev. Fluid Mech.* **24**, 235–279.

Shusser, M. & Gharib, M. 2000*a* Energy and velocity of a forming vortex ring. *Phys. Fluids* **12**, 618–621.

Shusser, M. & Gharib, M. 2000*b* A model for vortex ring formation in a starting buoyant plume. *J. Fluid Mech.* **416**, 173–185.

Shusser, M., Rosenfeld, M., Dabiri, J. O. & Gharib, M. 2006 Effect of time-dependent piston velocity program on vortex ring formation in a piston/cylinder arrangement. *Phys. Fluids* **18**, 033601.

Turner, J. S. 1962 The 'starting plume' in neutral surroundings. *J. Fluid Mech.* **13**, 356–368.

Weigand, A. & Gharib, M. 1997 On the evolution of laminar vortex rings. *Exp. Fluids* **22**, 447–457.

Yu, S. C. M., Ai, J. J. & Law, A. W. K. 2007 Vortex formation process in gravity-driven starting jets. *Exp. Fluids* **42**, 783–797.

Zhao, W., Frankel, S. H. & Mongeau, L. G. 2000 Effects of trailing jet instability on vortex ring formation. *Phys. Fluids* **12**, 589–621.